



# Automated Trajectory Planning and Analytical Improvement for Automated Repair by Robot-Guided Cold Spray

Marcel Lewke<sup>1</sup> · Hongjian Wu<sup>2</sup> · Alexander List<sup>2</sup> · Frank Gärtner<sup>2</sup> · Thomas Klassen<sup>2</sup> · Alexander Fay<sup>1</sup>

Submitted: 13 July 2023 / in revised form: 20 November 2023 / Accepted: 21 November 2023 / Published online: 18 December 2023  
© The Author(s) 2023

**Abstract** Cold spraying has emerged as a promising technique for the repair of metallic components. Manipulating the cold spray gun by industrial robots, referred to as robot-guided cold spraying, enables flexible and controlled material deposition. This work proposes a concept for automated planning of robotic cold spray paths and trajectories, enabling effective and efficient material deposition at specified repair locations. The concept incorporates predefined cold spray parameterizations and boundary conditions to provide the best possible material deposition for the individual repair application. The concept begins with the extraction of the volume to be filled. This volume is then sliced into suitable adaptively curved layers and converted into point clouds for path planning. Subsequently, the cold spray path is converted into a trajectory by adding a calculated spray velocity profile to produce the

required locally varying layer thicknesses. In addition, simulation of the material deposition and a kinematic analysis of the simulated trajectory are performed. These are utilized as performance indicators for assessing deposit quality and material efficiency, enabling the validation and improvement of the parameterized trajectory. Finally, the implementation of the entire concept is demonstrated by representative use cases. The results demonstrate successful automated path and trajectory planning by the proposed concept, contributing to the overall goal of automated repair of damaged components by cold spraying.

**Keywords** cold spray · repair · robotics · simulation · trajectory

## Introduction

The global consumption of resources and environmental impact are major challenges of modern times. Efficient component manufacturing and repair processes are essential to reduce global waste and energy consumption and to avoid prospective shortages in natural resources. New repair routes can be developed using additive manufacturing techniques to restore locally damaged areas of components with minimal use of resources. In this regard, cold spraying (CS) has emerged as an advantageous technique for repair applications and has already been successfully applied in various studies (Ref 1-3). As a solid-state technique, CS provides substantial advantages over thermal processes for depositing oxidation-sensitive materials (Ref 4). The advantages of CS include high deposition rates and low temperature input to the deposit material, resulting in possible high-quality repair (Ref 5, 6). However, to meet the required materials properties, the

---

This article is an invited paper selected from presentations at the 2023 International Thermal Spray Conference, held May 22-25, 2023, in Québec City, Canada, and has been expanded from the original presentation. The issue was organized by Giovanni Bolelli, University of Modena and Reggio Emilia (Lead Editor); Emine Bakan, Forschungszentrum Jülich GmbH; Partha Pratim Bandyopadhyay, Indian Institute of Technology, Karaghpur; Šárka Houdková, University of West Bohemia; Yuji Ichikawa, Tohoku University; Heli Koivuluoto, Tampere University; Yuk-Chiu Lau, General Electric Power (Retired); Hua Li, Ningbo Institute of Materials Technology and Engineering, CAS; Dheepa Srinivasan, Pratt & Whitney; and Filofteia-Laura Toma, Fraunhofer Institute for Material and Beam Technology.

---

✉ Marcel Lewke  
marcel.lewke@hsu-hh.de

<sup>1</sup> Institute of Automation Technology, Helmut Schmidt University, Hamburg, Germany

<sup>2</sup> Institute of Materials Science, Helmut Schmidt University, Hamburg, Germany

deposition must be precisely controlled with respect to primary CS process parameters, such as process gas temperature or process gas pressure. In addition, secondary parameters concerning the kinematics such as spray angle, spray distance, spray velocity and spray trace distance are crucial for successful deposition (Ref 7). These secondary, kinematic parameters describe the motion of the CS nozzle relative to the substrate and, like the primary parameters, directly affect the deposit properties. The spatial description of the impinging CS spot is given by the tool center point (TCP) of the robot's CS gun. Since terminology in the literature is often not consistent, definitions for the secondary, kinematic parameters are introduced according to the EN ISO 14917 standard (Ref 8). The transverse velocity of the robot TCP is referred to as the spray velocity in CS, which thus defines the relative velocity of the spray jet to the substrate. The spray angle defines the angle between the center line of the spray jet to the surface of the substrate. The distance between the face of the nozzle outlet and the substrate surface is defined by the spray distance. The spray trace distance defines the distance between the centers of adjacent spray traces and thus influences the overlap of spray traces and coating thickness per layer. Consequently, an increase of the spray trace distance results in a decrease of the overlap, assuming that the spray trace distance is always smaller than the trace width. The material efficiency specifies the deviation between the required material at the repair location and the actual deposited material and can be determined by the deviation between the nominal closing surface and the actual final deposit surface. The deviation can account for excess and missing material by considering the sign. High material efficiency thus implies efficient use of spray material and a low demand for surface finishing.

Results in literature indicate that best material properties can be expected at a spray angle orthogonal ( $90^\circ$ ) to the substrate surface (Ref 9–11). The required kinematic precision can be achieved by manipulation with industrial robots, here referred to as robot-guided CS. For controlled material deposition, this requires systematic path planning considering the specific boundary conditions by CS. With the spray path representing the geometric movement, and all of the mentioned kinematic parameters, the robot motion has a direct effect on the material deposition and thus on the deposit quality. To additionally enable path planning for additive volumetric buildup for repair by CS, a layer-by-layer approach is required. In order to solve these tasks, specific approaches are described in the literature. However, a comprehensive concept for automated and controlled manipulation of the material deposition is required. This concept should be adaptable to different geometries and parameterizations of the process.

Consequently, such a concept is addressed within the scope of this work.

For successful repair by CS, the damaged zone must be pre-machined to provide defined surface quality and geometries that meet the geometric boundary conditions for subsequent deposition (Ref 7, 12). The machining of the damaged zone inevitably results in a concave surface geometry. In this case, material deposition must cope with possible differences in layer thickness, adjustable spray distance and the limitation of the available working space. In this respect, trajectory planning becomes important for locally controllable material deposition by CS. Trajectories include an underlying path and the velocity and acceleration of the robot motion. In order to fill a concave surface, varying layer thicknesses need to be deposited to aim for near-net-shape filling. Near-net-shape refers to the manufacturing of components with final geometries and surfaces close to the predefined dimensions, which enables higher material efficiency and reduced efforts for surface finishing. Consequently, the spray velocity could be adapted to control the amount of material deposited per area per time. Nault et al. (Ref 13) state the importance of investigating the spray velocity for defined layer generation. The material deposition to a unit area per time is proportional to the powder feed rate and inversely proportional to the spray velocity. In case of excessive material buildup, the normal distribution of particle velocity in the gas jet results in accumulating formation of CS spots with steep sidewalls, which have a negative effect on the material deposition of subsequent layers (Ref 14). Thus, the amount of deposited material must be controlled accordingly within certain boundary conditions. In addition, as reported in the literature, a slow spray velocity results in a higher local heat input onto the substrate (Ref 15). This can be beneficial for coating properties, since coatings with low porosity can be obtained. Improved deposit properties at slow spray velocities can be attributed to locally attained higher effective surface temperatures (Ref 16). In contrast, locally higher surface temperatures can cause higher residual stresses, which can even result in delamination of the deposit (Ref 17). On the other extreme, applying excessively fast spray velocities can result in higher deposit porosity, which might not fulfill repair requirements (Ref 15, 17). Limits also apply to the powder feed rates. The literature reports that excessive powder feed rates can result in higher residual stresses and possible delamination of the coating (Ref 18). However, these effects, attributed to excessive material buildup, can be counterbalanced by an increased and matching spray velocity (Ref 18). In contrast, a too low powder feed rate is uneconomic due to higher gas consumption with less powder loading (ratio of mass flow rate of powder to the mass flow rate of gas) (Ref 19).

In addition to the deposit-related boundary conditions, also construction-related limits of the robot (e.g., joint limits) in combination with the given cavity dimensions under repair have to be considered and set the limits of the dynamic robot motion. In ideal, the dynamics of the robot should be used systematically for each unit area to ensure controlled heat input and efficient material deposition. Consequently, this results in a required parameter range for the best possible material deposition and the need to match all parameters for robot-guided CS accordingly. In order to consider all the influencing factors that have an impact on the quality and efficiency of the CS application, these complex interactions need to be systematically identified and integrated into a comprehensive concept.

Basic ideas for such a concept can already be found in the literature. Chen et al. (Ref 20) proposed an adaptive spiral trajectory for CS repair. An Archimedean spiral was used to ensure a constant distance between two adjacent spray traces. The trajectory was composed of two symmetrical Archimedean spirals. These were adjusted to the damage contour by linear transformation. For each target point, the spray velocity was adapted to the corresponding depth of the crater geometry by applying an approximate linear correlation between spray velocity and coating thickness. The results demonstrated a successful repair of the component with sufficient quality concerning porosity and bonding strength. However, the proposed spiral trajectory incorporated deviations from the orthogonal spray angle to the local surface. In the given example, the trajectory was functional for the use case, since the surface showed only small angular inclinations. For possibly larger inclinations, the local spray angle must be considered. Furthermore, the trajectory was repeated 30 times with a constant distance between CS gun and component, resulting in a constantly decreasing effective spray distance. No information was provided on the calculation of the required number of repetitions. For maintaining best possible CS conditions, it would be necessary to employ a layer-by-layer approach that considers the required number of layers with individually adapted spray distance.

Spiral trajectories were also used by Wu et al. (Ref 12). The authors proposed a framework for a complete repair process by CS. This framework contained a 3D scanning system for damage analysis and recognition, a damage pattern database and a robotic CS repair system. The data obtained by the 3D scanning system of the component were matched with existing damage patterns of the database for identifying standard defects. This information was used to determine a repair strategy, providing a suitable CS spiral trajectory for the material deposition. However, challenges remain related to the above-mentioned spiral trajectory method with respect to spray angle and spray distance.

In order to address all these tasks, this contribution proposes a comprehensive concept for automated path and trajectory planning for automated repair by robot-guided CS. This concept enables automated and controlled manipulation of the material deposition that allows adaptation to different geometries and parameterizations of the process. According to this concept, the paths and trajectories are planned based on the input geometry and the specific volume to be produced. In addition, the concept offers the capability to assess and improve the simulated trajectories with respect to suitability for required deposit quality and material efficiency. The concept is presented in the next section. The results section details the application of the concept with representative use cases. The results are then discussed from a broader perspective to finally conclude this work and to outline future research activities in ongoing projects.

## Concept

This section describes the concept for automated path and trajectory planning to enable automated repair by robot-guided CS. The section is divided into the following subsections: The first subsection contains the determination of the volume to be produced by CS. In addition, the volume is divided into adaptively curved layers to ensure the boundary condition of orthogonal spraying and the requirement of efficient material use. The second subsection covers automated path planning for each individual layer utilizing point clouds and normal vectors. Within the concept, this step allows to integrate different path algorithms. The third subsection contains the trajectory planning by adding a spray velocity profile to the generated path. This enables to control the amount of material deposition per area per time. In the fourth subsection, the validity of the determined trajectory is tested by a simulation of the material deposition. Here, the total accumulated deposited material as well as the difference to the nominal closing surface is determined. The fifth subsection covers the transfer of the generated trajectory to the robot environment, the subsequent simulation and the kinematic analysis. The implementation of the concept was performed in FreeCAD (version 0.20) (Ref 21) and RoboDK (version 5.5.0) (Ref 22). FreeCAD is a parametric 3D open-source computer-aided design (CAD) software, containing an interpreter based on the Python programming language. The proposed concept was implemented using Python scripts. A connection to the robot programming and simulation software RoboDK was established. This allows off-line simulation of generated robot programs, enabling testing of the programs before they are converted into robot control code for the real process. The concept additionally

contains the analysis of the simulated trajectories and iterative improvement of the parameterization until specified requirements are fulfilled. This analysis considers the robot kinematics and the material deposition, which serve as performance indicators for deposit quality and material efficiency. By considering the predefined specifications for the respective repair case, this step guarantees the most suitable parameterization of the process. Figure 1 depicts the flowchart of the entire concept.

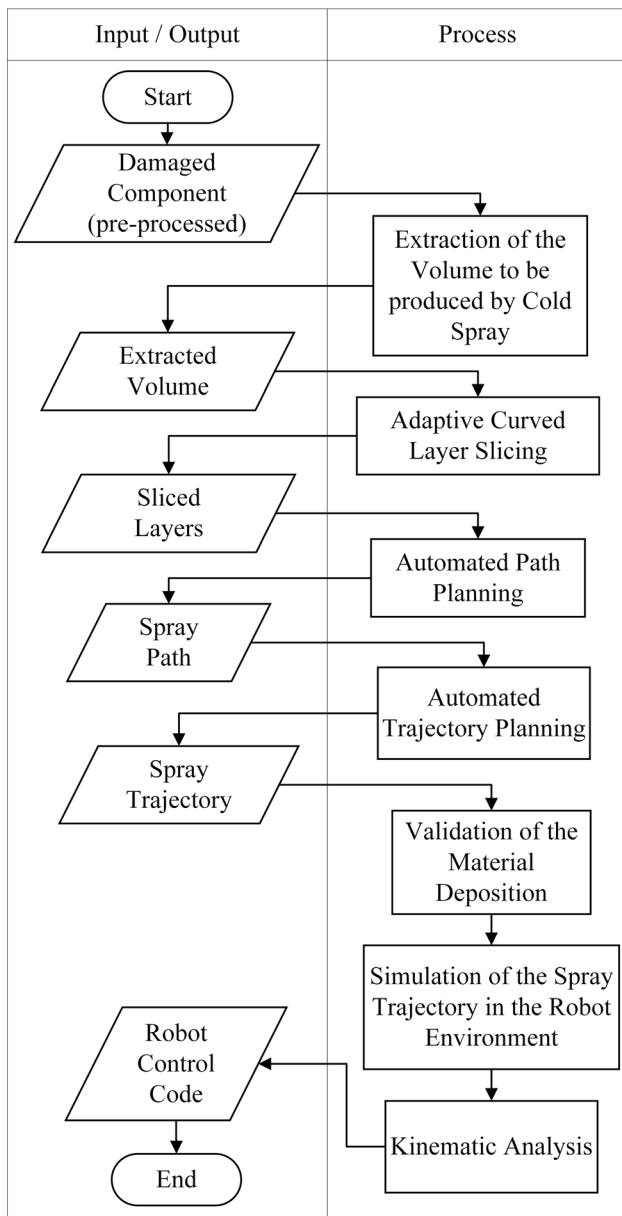


**Fig. 1** Flowchart of the concept for automated path and trajectory planning for automated repair by cold spray.

## Adaptive Curved Layer Slicing

In this work, it is assumed that a damaged surface has already been prepared for subsequent material deposition by pre-machining to remove the damage and by surface treatments (e.g., grit blasting) to improve adhesion. Furthermore, it is assumed that CAD models of the nominal and the actual components are present.

The first step requires the extraction of the volume to be restored by CS, as shown in Fig. 2. The missing volume can be determined by comparing the nominal and the actual digital model of the component using a Boolean comparison. Alternatively, the volume can be obtained by combining starting surface and closing spline surfaces. After determining the volume to be cold sprayed, the volume must be divided into suitable layers to provide the basis for the layer-by-layer buildup. The stacking of the sliced layers to form a volume is shown in Fig. 2(c). A layer is defined as the enclosed volume between two sliced surfaces. To ensure optimum deposit properties, an orthogonal spray angle ( $90^\circ$  to the local surface) must be incorporated. Due to the presence of concave surfaces during repair, curved layers are required to keep the spray angle orthogonal. In addition, filling of concave surfaces requires variations in local layer thicknesses. There are locations where more material is needed and locations where less material is needed to rebuild the volume. To save material during deposition and with the aim of producing near-net-shape deposits to reduce surface finishing, variable layer thicknesses are required. In summary, this results in the proposition of an adaptive curved layer slicing algorithm. The proposed algorithm requires the input of a starting surface and a closing surface to finally output the intermediate surfaces. The procedure involves the conversion of the starting surface into a point cloud (collection of discrete points in 3D space) by using the FreeCAD Points Workbench and a specified Euclidean distance. This Euclidean distance determines the spacing between points and influences the number of points in the point cloud. For a given geometry, a large Euclidean distance would result in a point cloud with a small number of points. In contrast, a small Euclidean distance would result in a point cloud with a large number of points. Consequently, the Euclidean distance affects the accuracy of the surface approximation to represent shape and curvature. A small Euclidean distance results in a high accuracy of the surface approximation and is used here accordingly. A normal vector is assigned to each point of the point cloud to represent orthogonality to the underlying surface. Based on this, the following surface is calculated by shifting the points along the normal vectors. The shift is scaled individually, based on the distance of the point to the closing surface of the volume. The scaling refers to the parameters of the

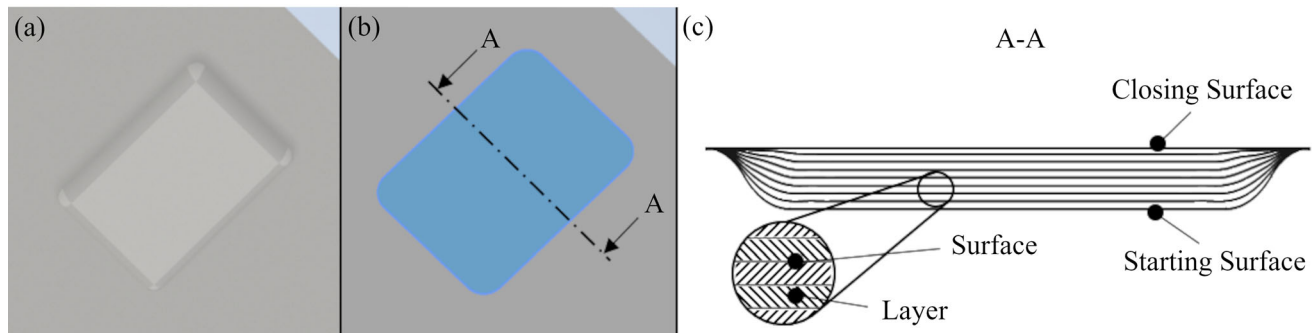


**Fig. 2** Result of adaptive curved layer slicing, (a) initial component surface, (b) extraction of the volume to be manufactured, (c) cross section of the resulting surfaces and layers

minimum and maximum layer thickness that should be produced. Consequently, points in larger distance to the closing surface (thick deposit required) are scaled more than points that are closer to the closing surface (thin deposit required). In this way, the adaptive approach of the algorithm guarantees variable layer thickness generation. After the creation of a following point cloud, this point cloud is transformed into a spline surface, containing points and normal vectors for repeating the algorithm. This loop is repeated until the closing surface of the volume to be filled is reached. Figure 2(c) shows the result of this slicing algorithm for a representative case.

### Automated Path Planning

The next step of the concept concerns automated path planning. A path represents a geometric sequence of movements for the defined robot TCP. The TCP defines the operating point of the CS gun, and thus, the spatial description of the impinging CS spot and incorporates a predefined spray distance.

For the purpose of automated path planning, each individually sliced surface has to be considered. A surface is now converted into another point cloud, again using the FreeCAD Points Workbench. However, this point cloud has a different role compared to the slicing step and therefore uses a different value for the Euclidean distance, providing the necessary flexibility for path planning. While in the slicing step the point cloud is used to create new surfaces and the Euclidean distance represents accuracy of the surface approximation, in path planning the point cloud represents the geometry of the robot path and the Euclidean distance corresponds to the specific CS spray trace distance. The latter is important in order to adjust to the CS spot dimensions and enables a controlled layer buildup. The normal vectors of this point cloud are used to align the TCP of the robot-guided CS gun and to guarantee an orthogonal spray angle. To sort the points of the point cloud, an algorithm is proposed to provide a suitable CS

path. This algorithm starts with determining a corner point of the point cloud and searches along the search direction for the nearest points based on minimum distances. To simplify the geometric calculations, the point positions are transformed to a local coordinate system. The orientation of the local coordinate system allows to simplify the search direction of the algorithm. This local search direction is directly influenced by the selected path pattern, zigzag or spiral. For a spiral path, the search direction is always adjusted at corner points until the spiral path is finally created. For a zigzag path, the search direction is adjusted more frequently to achieve the up-and-down movement. Each point in the point cloud that has already been included by the algorithm for path planning is excluded from further processing. This guarantees that every point is included only once in the path. The algorithm enables establishing path connections that are independent of the z-coordinate value. This allows creating paths over curved surfaces. Figure 3 depicts the output of a zigzag and a spiral path for a given input point cloud. To ensure smooth motion of the robot while following the path, RoboDK enables the use of motion blending. The motion blending parameter enables rounding of the executed robot motion at path edges to ensure smooth transitions between consecutive movements. Combining all the individual paths per surface creates an overall path for the total volume. This overall path incorporates transitions between the individual paths, where respective end points of the previous path correspond to the start point of the following one.

In order to ensure a smooth robot motion, the TCP orientations given by the normal vector sequence should include smooth transitions. When depositing material on complex surfaces with possible changes in the path direction, sudden changes in the orientation of the TCP may occur. Although orthogonality is ensured for the respective path points, the sudden changes can result in unnecessary accelerations of the robot joints to adjust to the next robot configuration. Such jerky motion can be unfavorable for the deposit quality (Ref 23). As stated, the best material

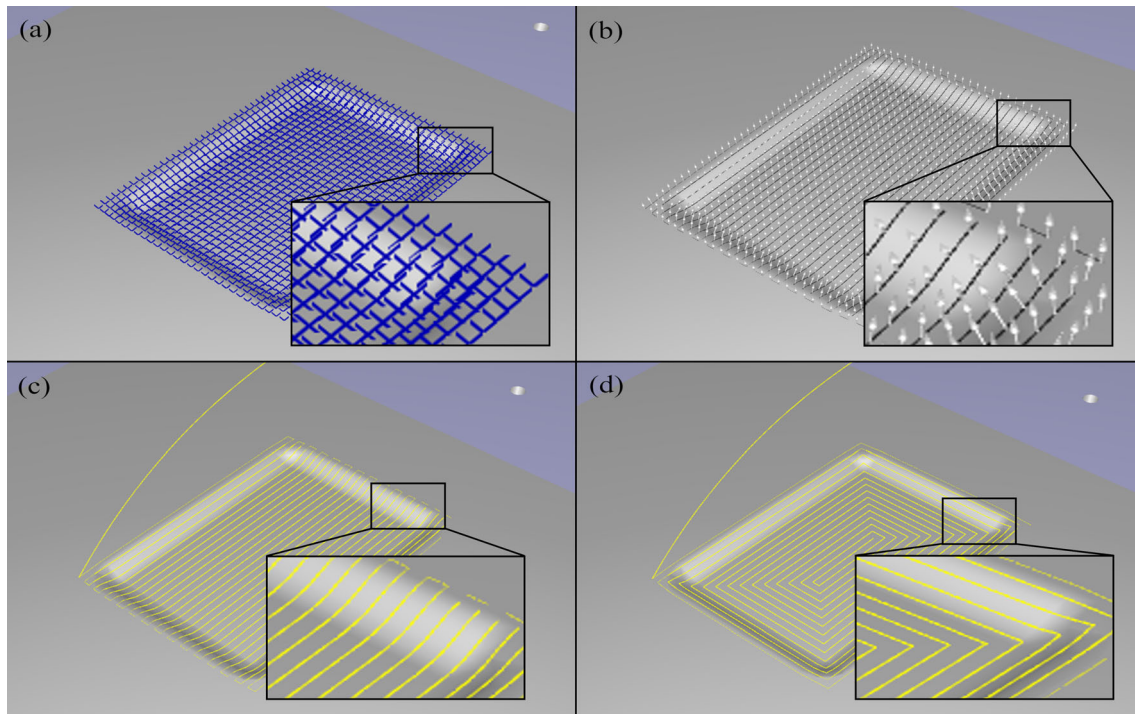


**Fig. 3** Example of path planning for a deposit layer, (a) point cloud, (b) normal vectors, (c) zigzag path, (d) spiral path.

properties are obtained by an orthogonal spray angle to the substrate surface. However, literature indicates that small deviations from an orthogonal spray angle could be tolerable, depending on the respective application (Ref 9). This results in a tradeoff between smoothness and strict orthogonality, both influencing the quality. For automated path planning, an algorithm was implemented that applies normal vector smoothing using a sliding window approach. In a loop, a single normal vector is selected and compared with the previous and following normal vector with respect to the angle change. By choosing the magnitude of smoothing, the angular changes are minimized, ensuring smooth transitions between changes in TCP orientations. The averaged angular deviations from orthogonality are calculated and allow the appropriate selection of the smoothing magnitude.

### Automated Trajectory Planning

In this step, the planned path is converted into a trajectory. The trajectory now includes the spray velocity, which is calculated based on the sliced surfaces. The required layer thickness assigned to each point defines the locally required spray velocity. The spray velocity is thus the parameter for ensuring variable layer thicknesses.

The spray velocities are calculated based on the respective actual working surface and the subsequently following support surface. The normal vectors from the

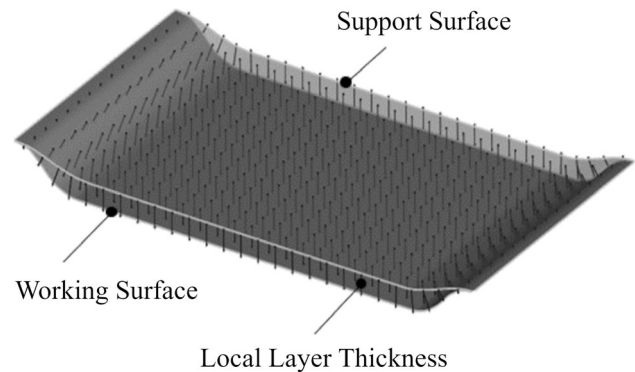


**Fig. 4** Example for determining local layer thicknesses between the working surface and the support surface

path of the working surface are used to determine the intersection points with the support surface, resulting in cutting vectors. The length of the cutting vector  $h_l$  represents the local layer thickness for an individual point of the respective layer. A representative illustration for determining the local layer thicknesses is shown in Fig. 4. The lower surface always represents the working surface for the layer to be produced. The locally required layer thickness  $h_l$  is then converted into a value for the spray velocity. For the calculation of the spray velocity, represented as  $v_{gun}$ , the equation proposed by Nardi et al. (Ref 24) is applied:

$$v_{gun} = \frac{\varphi \cdot DE}{d \cdot \delta \cdot h} \quad (\text{Eq 1})$$

In Eq 1,  $\varphi$  denotes the powder feed rate,  $DE$  the deposition efficiency,  $d$  the nozzle exit diameter (corresponding to CS spot diameter),  $\delta$  the material density and  $h$  the line height. For the line height  $h$ , the corresponding calculated local layer thickness  $h_l$  is inserted, while the other parameters remain constant. The corresponding calculation is repeated iteratively until every point of the path contains a spray velocity value, resulting in the final trajectory with the corresponding spray velocity profile. The generated trajectories could then be transferred to the robot simulation environment or better, before, assessed with regard to material deposition.

### Modeling and Simulation of the Material Deposition

The simulation of the material deposition serves to check the validity of the path and the trajectory before further processing is performed by the robot. Sufficient accuracy for the deposit buildup must be ensured to verify the trajectory concerning complete filling of the cavity. The modeling of the material deposition assumes a Gaussian function to represent local CS spots. The material deposit is assumed to be normally distributed, due to the normal distribution of the number and velocities of particles in the gas jet. To relate the height of the Gaussian function to the parameterization of the process, the determined local layer thickness is set as the amplitude (peak height) of the Gaussian function. This Gaussian function incorporates height scaling, according to the spray velocity. A high spray velocity results in a low height of the CS spot and vice versa. The diameter of the CS spot corresponds to the nozzle exit diameter. In addition, an orientation of the Gaussian function corresponding to the local surface curvature and the underlying normal vector is included to account for the spray angle.

Figure 5 illustrates the simulation of material deposition for the example of coating a flat surface. Figure 5(a) shows the flat surface before material deposition. Overlapping of single Gaussian functions (Fig. 5b), representing CS spots, forms CS traces (Fig. 5c). The overlap of adjacent CS traces forms the deposited CS layer (Fig. 5d). The amount of overlap is determined by the set spray trace distance. Finally, overlaying of possible multiple CS layers results in the total deposited volume. The modeled material deposition in Fig. 5(d) also illustrates the edge losses occurring in CS, which are caused by the normal distribution characteristics.

In order to quantitatively evaluate the geometric match of the final material deposit, the mean deviation of the final deposit surface to the nominal closing surface is calculated, which represents material efficiency. The mean deviation is determined by calculating the signed distances between sample points on the final deposit surface and the nominal

closing surface. The sum of these distances is then averaged to obtain an overall measure of deviation. This mean deviation has a sign and can represent both excess material with a positive sign as well as missing material with a negative sign. Although in repair applications the cavity should be at least completely filled, so that a small amount of excess material is preferable.

### Simulation and Kinematic Analysis of the Robot Trajectory

In this step, the transfer of the trajectory to the robot simulation environment, details on the subsequent robot simulation, and the kinematic analysis of the robot motion are presented. The digital model of the robot cell must include the executing robot, all relevant tools (e.g., CS gun) and other peripherals. During the setup of the CS robot, the specified TCP defines the operating point of the impacting material, considering the required spray distance. This spray distance is kept constant for each path point and each applied layer, respectively, to maintain best possible conditions for material deposition. Figure 6 shows an example of a robot trajectory simulation for a flat substrate coating with a zigzag path.

The simulation of the trajectory is performed in the robot simulation environment and, together with the kinematic analysis, serves to verify the feasibility of the robot motion. Singularities and collisions of the robot must be avoided. In addition, the kinematic analysis of the simulated robot motion allows indirect conclusions about the deposit quality by checking the kinematics.

The kinematic analysis considers position, velocity, acceleration and jerk for the TCP within the Cartesian space and for the robot joints, respectively. RoboDK allows to read out joint positions at discrete time steps. By using the forward kinematics (Ref 25), the position of the TCP was determined for each respective joint configuration. Subsequently, the velocity, acceleration and jerk were calculated by differentiation with the respective time steps. The kinematic analysis checks whether the robot can provide the needed spray velocity profile that was calculated based on the targeted local layer thicknesses and the set powder feed rate. The prospective feasibility depends on the dimensions of the cavity and the joint limits of the respective robot, which determines the dynamic of the robot motion. Results are presented in the form of a graphical representation of the kinematics and by calculated mean values. The mean value of the spray velocity allows to derive estimates with respect to local heat input and possible consequences for residual stress development. The influence of the spray velocity on the effective surface temperature can also affect the porosity of the deposit. Furthermore, acceleration and jerk can be considered as

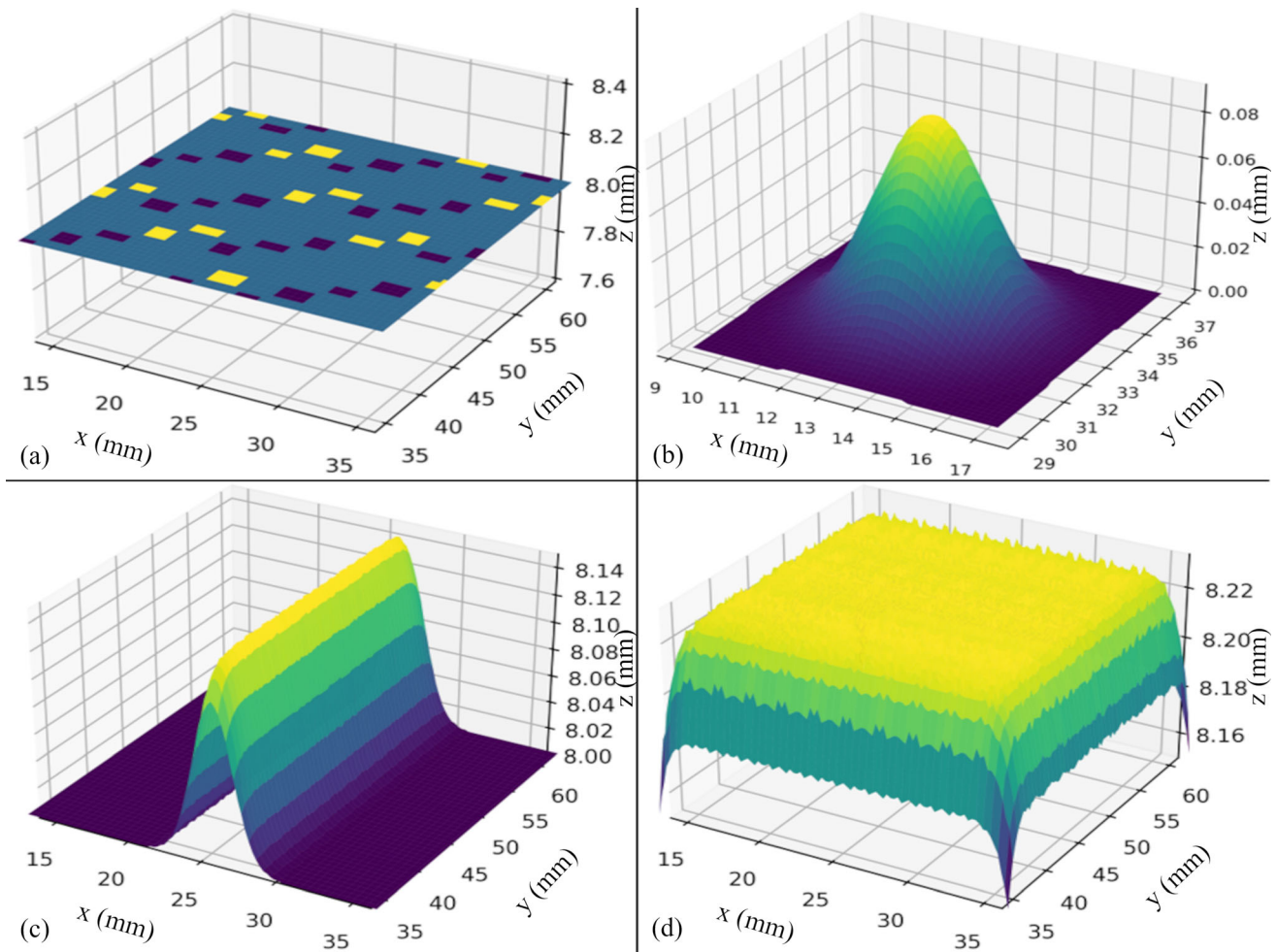


**Fig. 5** Example for modeling of the material deposition, (a) surface before material deposition, (b) illustration of a cold spray spot, (c) illustration of a cold spray trace, (d) surface after material deposition

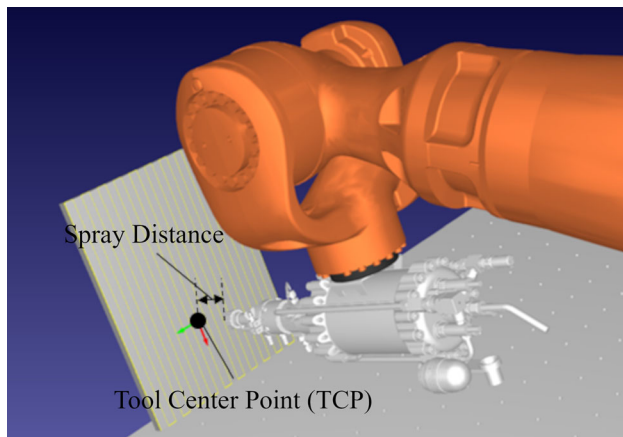


**Fig. 6** Example of a robot trajectory for a flat substrate coating in the robot simulation environment

indicators of having a smooth motion, which is important for a steady handling of material deposition and thus low deviations in local layer buildup.

As a feasibility study, the following example presents the coating with aluminum alloy 6061 powder on a flat substrate with 250 mm length and 200 mm width. The desired layer thickness was set to 0.2 mm. In addition, a powder feed rate of 50 g/min, a deposition efficiency of 70%, a CS spot diameter of 8 mm, and a calculated spray velocity profile of ideally constant 135 mm/s were set. The resulting trajectory was simulated and kinematically analyzed. Figure 7(a) shows the resulting kinematics for the TCP. Accordingly, in Fig. 7(b), the kinematics for the joints are displayed. A Butterworth filter is used to eliminate the noise in the profiles. The results illustrate the successful application of the desired trajectory for the coating example. The mean spray velocity with a value of  $131.87 \pm 21$  mm/s is within the required parameter range. The local variations



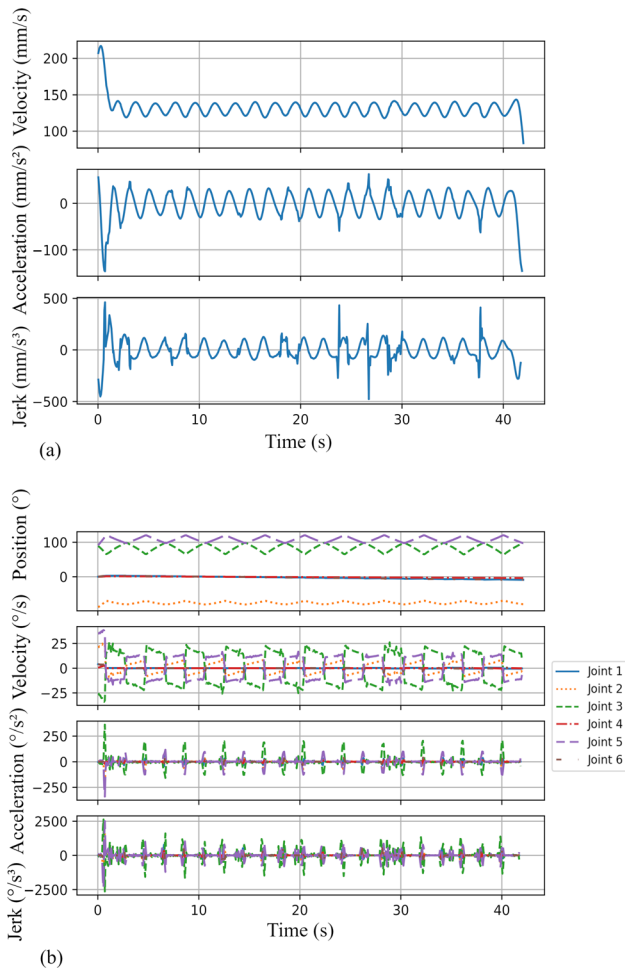


**Fig. 7** Kinematic analysis of the simulation example for a flat substrate coating, (a) TCP values, (b) joint values

result from the directional changes of the path. The accelerations and jerks are within an acceptable range and do not impede with the deposition process.

After successful simulation and respective kinematic analysis proving the suitability of the robot trajectory for the repair process, the robot simulation environment allows the generation of control code. A postprocessor translates the generated robot program into the required robot language. This enables the transfer of the control code to a real robot to perform the deposition process. Finally, after the successful simulation of the robot trajectory, the application of the entire concept must be tested for representative use cases.

## Results

This section presents the results of applying the overall concept to representative use cases. The presented component and damage geometries could serve as examples of aircraft components. To validate the flexible use of the

repair concept, examples concerning the repair of a planar cavity and a curved cavity are utilized. The terms *planar* and *curved* are used to describe the local surface features of the component and to simplify the classification of the cavities. The planar cavity and the curved cavity both contain rounded edges. While *planar* refers to a cavity on a primarily planar component surface and a planar closing surface, *curved* refers to a cavity on a primarily curved component surface and a curved closing surface. The proposed concept enables automated trajectory planning and simulation of the process, which includes the simulation of the material deposition and the kinematic analysis of the robot motion to derive performance indicators. On this basis, the following steps in the concept aim to automatically analyze and improve the parameterization of the process iteratively with respect to the given boundary conditions, the cavity dimensions and the robot limits. (i) The first step involves iteration of the spray trace distance. By varying the spray trace distance, the amount and height of the deposited material are influenced in a controlled manner and allow to minimize the deviation to the nominal closing surface to ensure material efficiency. (ii) The second step involves iteration of the powder feed rate to control the resulting spray velocity profile. This setting has an influence on local surface temperature and the associated effects on cohesive coating strengths as well as on residual stresses within the deposit. Particularly for the latter, the spray velocity must be selected appropriately to ensure the required deposit quality. In this concept, possible parameter ranges for spray trace distance and powder feed rate as well as the desired target values for final deposit deviation and mean spray velocity need to be defined as requirements, including termination criterions.

The spray trace distance was set in the range of 2–4 mm with a step size of 0.2 mm. The powder feed rate was set to range from 10–100 g/min with a step size of 5 g/min. Desired target values for mean final deposit deviation and mean spray velocity by kinematic analysis were set to 0.1–0.3 mm and 100–140 mm/s, respectively. The positive sign of the mean final deposit deviation here is to ensure complete filling of the cavity by a small amount of excess material and to include a tolerance margin for post-machining. For the adaptive curved layer slicing, a maximum layer thickness of 0.4 mm was set. A spiral path was selected for path planning. The CS spot diameter was set to 8 mm, and aluminum alloy 6061 was selected as deposit material. The deposition efficiency was set to 70%. In combination with the given material density and the set powder feed rate, the calculated required spray velocity profile provides the buildup of the individual layers and the required variable layer thicknesses by the desired dynamics in the spray velocities. The boundary conditions for setting the powder feed rate range between as high as possible and

as low as necessary without influencing particle acceleration. The spray velocity should range between as low as possible and as high as necessary, to incorporate targeted deposit buildup, local heat input and associated residual stresses. Since for the controlled repair, both objectives for the powder feed rate and the spray velocity work in opposing directions for the generation of a specific layer thickness, a corresponding tradeoff must be established to match these parameters accordingly. Thus, in order to compensate for the increasing material deposition rate for a given layer thickness, in this concept, an increase in the powder feed rate is matched by a simultaneous increase in the spray velocity, while both must fulfill the process-related boundary conditions. The limit for maximum spray velocity was set to 300 mm/s to aim for adequate surface temperature and avoid possible negative effects on porosity. Normal vectors smoothing was applied to cope with possible minor approximation errors by slicing and provide a smooth robot motion.

### Repair of a Planar Cavity

The example in Fig. 8 shows the repair of a volume with planar starting surface with rounded edges and planar closing surface. The cavity had a length of 27 mm and a width of 21 mm. The maximum depth of the cavity was 1.26 mm, resulting in a total of 4 layers to produce according to adaptive curved layer slicing.

In the first step, the spray trace distance was varied and the resulting material efficiency was checked. An increasing spray trace distance causes a decrease of the final deposit height due to the increased distance between the spray traces and therefore lower amount of overlapping. However, the amount of overlap must not be too low, otherwise areas will form in the final deposit where the cavity is not completely filled. Figure 9 shows the iteration steps for the spray trace distance to reach final deposit

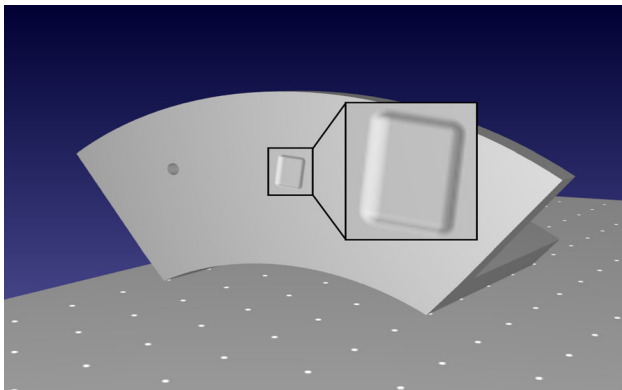


**Fig. 8** Example of a planar cavity before repair in the robot simulation environment

surface close to the closing surface under efficient material use. The initial spray trace distance was set to 2 mm with an increase per iteration step of 0.2 mm. The iterative simulations terminate automatically when the predefined mean target values are reached. The resulting spray trace distance in iteration step 5 was 2.8 mm. This resulted in a mean deviation to the closing surface of 0.3 mm, so that the resulting spray trace distance was parameterized for the further process. The decreasing standard deviation indicates a more uniform material deposition. Next, the powder feed rate was varied to check the resulting mean spray velocity. Starting with the highest powder feed rate, the highest mean spray velocity is assigned to cope with the demanded material deposition rate. Thus, decreasing the

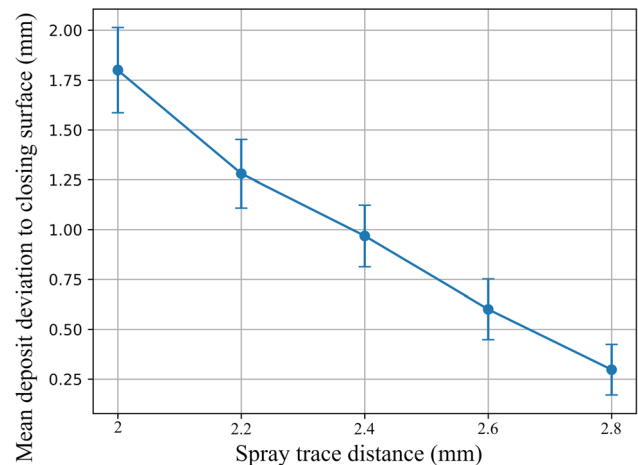


**Fig. 9** Deviation of the final deposit surface to the nominal closing surface vs. increasing spray trace distance for the planar cavity. The change in spray trace distance is described by the iterations and ends when the termination criterion is fulfilled

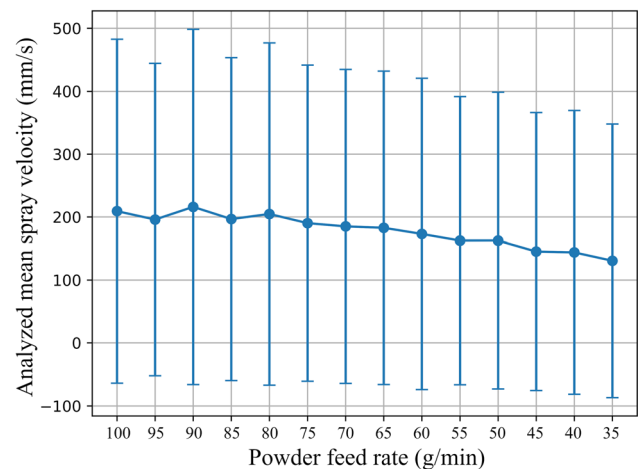


**Fig. 10** Mean spray velocity by kinematic analysis vs. decreasing powder feed rate for the planar cavity. The change in powder feed rate is described by the iterations and ends when the termination criterion is fulfilled

powder feed rate with proceeding iteration steps consequently results in a decrease in the mean spray velocity. Figure 10 shows the corresponding graph. The high standard deviations of the data in Fig. 10 are a consequence of the intentional dynamics. At the edges, faster local spray velocities are intended to deposit thinner local layer thicknesses, while slower local spray velocities are used in the center of the cavity. This is required to achieve shape accuracy at rounded edges in terms of material efficiency. It should be noted that reaching negative spray velocities within the symmetric range of standard deviations, shown in Fig. 10, has no physical meaning for the process. The spray velocities are given as absolute values without directions and are consequently always positive. Starting from the set target value, iteration step 14 with a powder feed rate of 35 g/min resulted in a mean spray velocity of 130.7 mm/s and was thus parameterized. In addition, there is a tendency that decreasing the powder feed rate additionally contributes to an improvement of the material efficiency, which can be explained by the set limit of the maximum spray velocity of 300 mm/s. This set spray velocity limit is not high enough for the highest powder feed rates to achieve good material efficiency, but was maintained due to higher prioritization of heat input, effective surface temperature and thus deposit quality. At the same time, an increase in spray trace distance results in a small increase in mean spray velocity. This can be explained by fewer passes per layer that follow for the cavity surface at its fixed dimensions. Fewer passes result in fewer turning points for the robot, and thus less deceleration.

The example was next set with the determined parameters for spray trace distance and powder feed rate. Results of the planar cavity example are depicted in Fig. 11. Figure 11(a) shows the calculated spray velocity profile to specifically control the amount of deposited material. Figure 11(b) depicts the generated final trajectory in RoboDK. In Fig. 11(c) and (d), the material deposition is illustrated. Calculated spray velocities for the controlled material deposition resulted in a minimum value of 44.69 mm/s, a maximum value of 300 mm/s, and a mean value of 174.49 mm/s. This dynamic in the profile of the calculated spray velocity ensures the generation of variable layer thicknesses and controlled material deposition. Smoothing the normal vectors resulted in a mean deviation from orthogonality of  $2.78^\circ$ . The mean spray velocity determined by the kinematic analysis was 146.41 mm/s, which is below the calculated value of 174.49 mm/s. This can be explained by the dynamics of the robot not being sufficient to follow the spray velocity profile precisely for the given dimensions of the cavity. The mean deviation to the closing surface was  $0.06 \pm 0.23$  mm. In summary, the results prove the successful application of the proposed

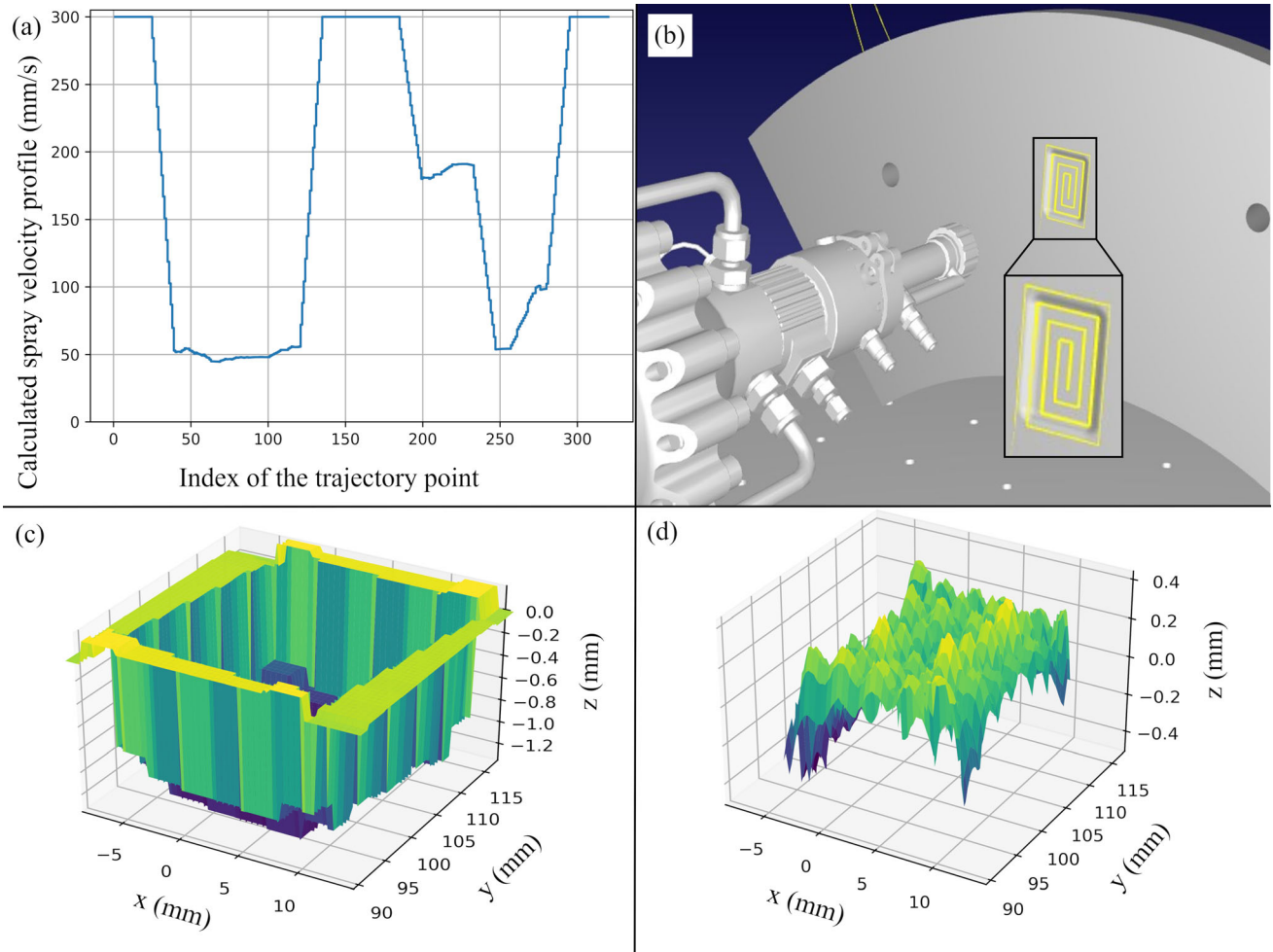
concept, as the evaluated parameters are within an acceptable range of the requirements.

### Repair of a Curved Cavity

In this example, illustrated in Fig. 12, the starting surface with rounded edges and the closing surface were both curved. The curved cavity had a length of 56 mm and a width of 19 mm. The maximum depth along the normal direction of the cavity was 1.4 mm. The adaptive curved layer slicing resulted in a total of 4 layers for filling the cavity.

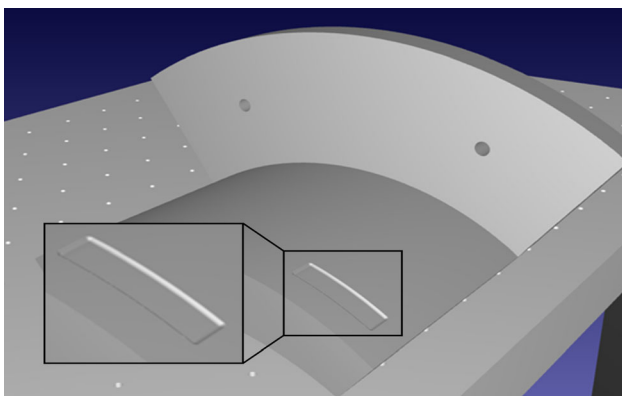
First, the spray trace distance and powder feed rate were varied to fulfill the requirements. Figure 13 shows the mean deviation between final deposit surface and nominal closing surface over the iterated spray trace distance for the curved cavity example, which represents the material efficiency. In iteration step 4, the spray trace distance was 2.6 mm and resulted in a mean deviation from the closing surface of 0.17 mm. This spray trace distance value was consequently parameterized for the following process. Figure 14 shows the correlation between mean spray velocity and the powder feed rate in the sequence of iteration steps. The suitable kinematically analyzed mean spray velocity of 126.7 mm/s was achieved at a powder feed rate of 25 g/min, examined in iteration step 16. Both of these examined parameters were set in the following process.

Figure 15 shows the results of the curved cavity example by applying the determined parameters for spray trace distance and powder feed rate. The calculated spray velocity profile and the generated final trajectory in RoboDK are shown in Fig. 15(a) and (b), respectively. The material deposition is illustrated in Fig. 15(c) and (d). The calculated spray velocities resulted in a minimum value of 31.9 mm/s, a maximum value of 300 mm/s, and a mean value of 134.73 mm/s. In comparison with the previous repair example, the lower mean spray velocity indicates the higher mean layer thicknesses that inevitably result with the same number of layers and a deeper cavity. Normal vector smoothing resulted in a mean deviation to orthogonality of  $2.14^\circ$ . The determined mean spray velocity by the kinematic analysis was 122.17 mm/s, which is in range to the calculated value of 134.73 mm/s. Due to the larger dimensions of the cavity compared to the previous example, larger distances of acceleration for the robot were given. This enabled the robot to follow the calculated spray velocity profile more precisely. The mean deviation to the closing surface was  $0.08 \pm 0.5$  mm. In summary, the results demonstrate the successful application of the concept for CS repair for a planar and curved cavity example, indicating the utility and flexibility of this concept.



**Fig. 11** Simulation results of the concept for the planar cavity, (a) calculated spray velocity profile, (b) final spiral trajectory in the robot simulation environment, (c) planar cavity before material

deposition, (d) material deposit in the planar cavity. Please note the different scales in the xy-plane and the z-axis of the thickness



**Fig. 12** Example of a curved cavity before repair in the robot simulation environment

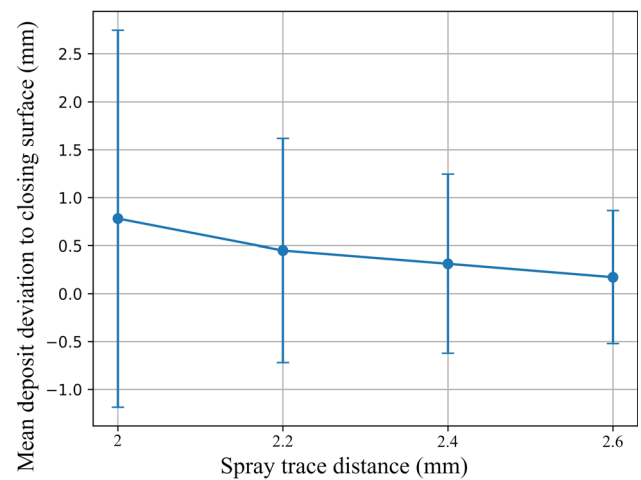


**Fig. 13** Deviation of the final deposit surface to the nominal closing surface vs. increasing spray trace distance for the curved cavity. The change in spray trace distance is described by the iterations and ends when the termination criterion is fulfilled

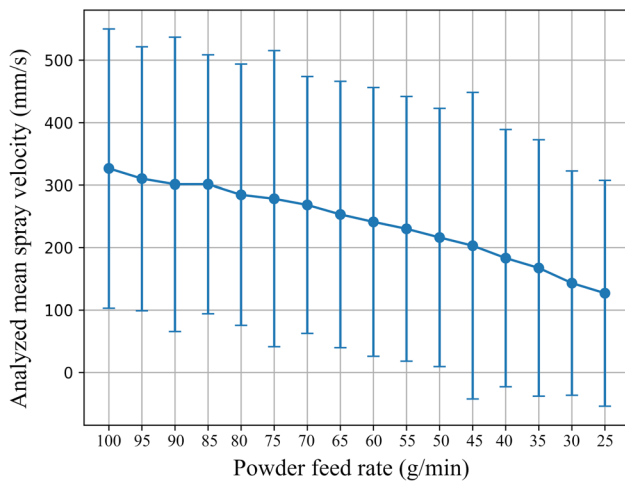


**Fig. 14** Mean spray velocity by kinematic analysis vs. decreasing powder feed rate for the curved cavity. The change in powder feed rate is described by the iterations and ends when the termination criterion is fulfilled

**Discussion**

The present work provides a concept for automated path and trajectory planning for repair by robot-guided CS. The individual steps of the concept enable to adapt material deposition to cavity geometries and to convert it into a suitable robot motion, while considering the secondary, kinematic parameters as well as efficient material use. The concept additionally includes an iterative analysis and improvement of the parameterization, which ensures a suitable repair process. Overall, the presented results demonstrate the feasibility of the concept. The parameterization illustrated here is specific to the repair examples. However, the overall concept offers the flexibility to adjust the parameterization by incorporating different parameters, boundary conditions, and desired target values to consider variable geometries and repair requirements.

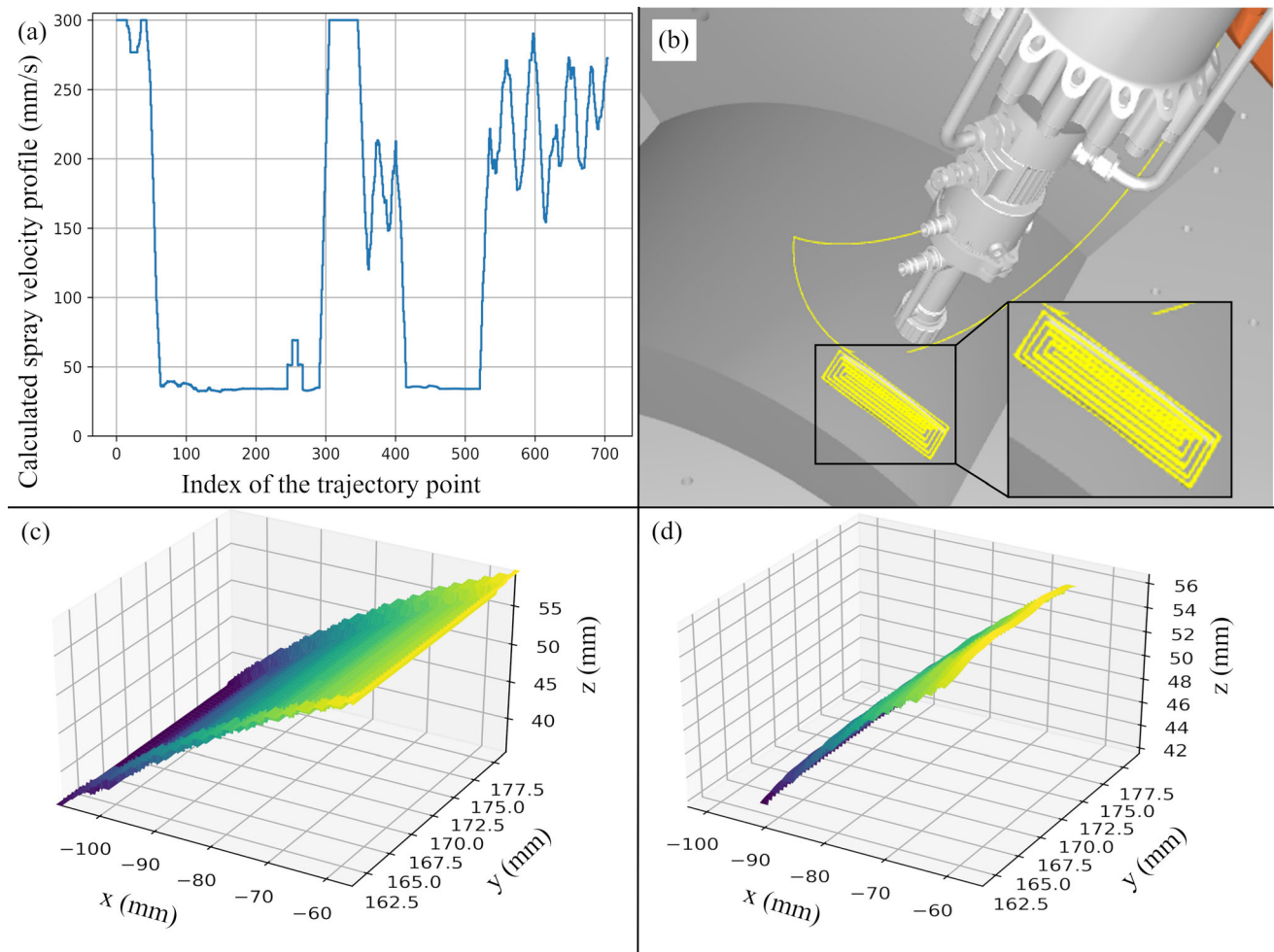


**Fig. 15** Simulation results of the concept for the curved cavity, (a) calculated spray velocity profile, (b) final spiral trajectory in the robot simulation environment, (c) curved cavity before material

deposition, (d) material deposit in the curved cavity. Please note the different scales in the xy-plane and the z-axis of the thickness

However, the current concept contains certain simplifications and assumptions, which are now under practical investigation. Thus, current investigations refer to real cold spray experiments to validate the concept. These analyses concern the dynamics (forces, inertia, and friction) of the robot, which are so far not included in the simulation of the kinematics of the robot motion. In addition, it should be clarified whether changes of the spray trace distance might cause wavier surface topographies that can have disadvantages on the subsequent material buildup and shape accuracy, which is not yet included in the concept. Surface waviness would impair shape accuracy and might cause local deviations from orthogonal spray angle. Apart from above, surface waviness can also pose a challenge to the current metric for evaluating cavity filling. The mean deviation might include a balancing effect between locally missing and locally deposited excess material zones, which cannot be detected. To address this issue, a refined approach could assess the pointwise deviation between the final deposit surface and the nominal closing surface. Integrating pointwise validation into the iterative nature of the concept in combination with additional restrictions of local deviations could avoid compensation of deviations and thus ensure precise material deposition and associated cavity filling. In addition, the spray trace distance might also affect the effective surface temperature. A high overlap at small spray trace distance would result in a more concentrated cumulative heat input and thus higher surface temperature. Conversely, a small overlap would result in a more distributed heat input and lower surface temperature. Consequently, the spray trace distance should be specifically controlled in terms of thermal management and finding the adequate balance between surface heating and induced thermal stresses. As a further influencing variable, the layer thickness could be considered in the slicing step to also specifically control the resulting process. Thinner layer thicknesses would correspond to faster spray velocities and thus less local heat input. This could be beneficial for inducing fewer thermal stresses. On the other hand, deposit qualities might be affected by missing deformation of less softened surfaces. In addition, the use of fast spray velocities also depends on the dynamic capabilities of the robot. The other extreme could be investigated by higher layer thicknesses, resulting in slower spray velocities. In conclusion, it is necessary to apply the presented concept by CS laboratory experiments and to investigate the influence of trajectories on relevant deposit properties.

## Conclusion and Outlook

Robot-guided cold spraying provides flexible control and automation of the material deposition. This enables the application of cold spraying as a repair technique for locally damaged components. However, to enable precise material deposition, a concept for handling the cold spray gun by industrial robots is required. In order to achieve the best possible material deposition, corresponding parameterization of the cold spray process and the handling robot is required. In addition, the complexity of choosing the right parameterization requires a comprehensive concept for planning, simulation and execution of the repair process.

This work presents a concept for automated path and trajectory planning for the automated repair of damaged components by cold spraying. The concept includes flexible path and trajectory planning, adaptable to different damage shapes, component geometries and cold spray parameterizations. Material deposition and robot kinematics are simulated and analyzed as performance indicators for required deposit quality and efficient material use to validate the suitability of the trajectory. Variable parameterizations and boundary conditions are considered with respect to the required high quality of cold spraying as well as the efficient use of the deposition material. In this process, predefined boundary conditions are incorporated to provide the most suitable trajectory for the individual repair case. The results demonstrate the successful application of the presented concept for cavity examples in flat and curved surface components.

Next steps under progress concern practical validation of this concept by laboratory cold spray experiments. In addition to geometric conformity, the experiments and subsequent analyses will aim to investigate the influences of the trajectories on deposit microstructures and properties. The research activities also focus on improving the automation of the repair process by robot-guided cold spraying using mathematical optimization. Integrating mathematical optimization will enable more sophisticated objectives and constraints, such as considering pointwise deviation to ensure accurate filling of cavities and directly accounting for possible robot limitations. This integration of mathematical optimization is expected to further improve the quality of deposits and material efficiency in robot-guided cold spraying. This concept will then be integrated into an overall robot-guided cold spray repair system and, with the integration of all supporting sub-processes, enable an automated repair process by cold spraying. Apart from that, most of the process routines can

also be adapted for cold spray additive manufacturing, opening up a new branch of process automation.

**Acknowledgments** The authors gratefully acknowledge the financial support in the frame of the project “CORE – Computer-based Refurbishment” funded by dtcc.bw – Digitalization and Technology Research Center of the Bundeswehr. dtcc.bw is funded by the European Union – NextGenerationEU.

**Funding** Open Access funding enabled and organized by Projekt DEAL.

**Open Access** This article is licensed under a Creative Commons Attribution 4.0 International License, which permits use, sharing, adaptation, distribution and reproduction in any medium or format, as long as you give appropriate credit to the original author(s) and the source, provide a link to the Creative Commons licence, and indicate if changes were made. The images or other third party material in this article are included in the article’s Creative Commons licence, unless indicated otherwise in a credit line to the material. If material is not included in the article’s Creative Commons licence and your intended use is not permitted by statutory regulation or exceeds the permitted use, you will need to obtain permission directly from the copyright holder. To view a copy of this licence, visit <http://creativecommons.org/licenses/by/4.0/>.

## References

1. M. Yandouzi, S. Gaydos, D. Guo, R. Ghelichi and B. Jodoin, Aircraft Skin Restoration and Evaluation, *J. Therm. Spray Tech.*, 2014, **23**(8), p 1281-1290.
2. V. Champagne and D. Helfritsch, Critical Assessment 11: Structural Repairs by Cold Spray, *Mater. Sci. Technol.*, 2015, **31**(6), p 627-634.
3. C.A. Widener, M.J. Carter, O.C. Ozdemir, R.H. Hrabec, B. Hoi-land, T.E. Stamey, V.K. Champagne and T.J. Eden, Application of High-Pressure Cold Spray for an Internal Bore Repair of a Navy Valve Actuator, *J. Therm. Spray Tech.*, 2016, **25**(1-2), p 193-201.
4. H. Assadi, H. Kreye, F. Gärtner and T. Klassen, Cold Spraying – a Materials Perspective, *Acta Mater.*, 2016, **116**, p 382-407.
5. M.E. Lynch, W. Gu, T. El-Wardany, A. Hsu, D. Viens, A. Nardi and M. Klecka, Design and Topology/Shape Structural Optimisation For Additively Manufactured Cold Sprayed Components, *Virtual Phys. Prototyp.*, 2013, **8**(3), p 213-231.
6. W. Li, K. Yang, S. Yin, X. Yang, Y. Xu and R. Lupoi, Solid-State Additive Manufacturing and Repairing by Cold Spraying: a Review, *J. Mater. Sci. Technol.*, 2018, **34**(3), p 440-457.
7. S. Yin, P. Cavaliere, B. Aldwell, R. Jenkins, H. Liao, W. Li and R. Lupoi, Cold Spray Additive Manufacturing and Repair: Fundamentals and Applications, *Addit. Manuf.*, 2018, **21**, p 628-650.
8. EN ISO 14917: Thermal Spraying - Terminology, Classification (ISO 14917:2017).
9. K. Binder, J. Gottschalk, M. Kollenda, F. Gärtner and T. Klassen, Influence of Impact Angle and Gas Temperature on Mechanical Properties of Titanium Cold Spray Deposits, *J. Therm. Spray Tech.*, 2011, **20**(1-2), p 234-242.
10. Q. Blochet, F. Delloro, F. N’Guyen, F. Borit, M. Jeandin, K. Roche, and G. Surdon, (2014) Influence of Spray Angle on Cold Spray with Al For the Repair of Aircraft Components. In: *Thermal Spray 2014: Proceedings from the International Thermal Spray Conference*, (Barcelona, Spain), 2014, p 69-74.
11. Li, C. J., W. Y. Li, Y. Y. Wang, and H. Fukunuma (2003) Effect of Spray Angle on Deposition Characteristics in Cold Spraying, *Thermal Spray Advancing the Science and Applying the Technology*, B.R. Marple and C. Moreau, (Eds.), ASM International, Orlando, FL, 2003: 91-96
12. H. Wu, S. Liu, X. Xie, Y. Zhang, H. Liao and S. Deng, A Framework for a Knowledge Based Cold Spray Repairing System, *J. Intell. Manuf.*, 2022, **33**, p 1639-1647.
13. I.M. Nault, G.D. Ferguson and A.T. Nardi, Multi-Axis Tool Path Optimization and Deposition Modeling for Cold Spray Additive Manufacturing, *Addit. Manuf.*, 2021, **38**, 101779.
14. J. Pattison, S. Celotto, R. Morgan, M. Bray and W. O’Neill, Cold Gas Dynamic Manufacturing: A Non-Thermal Approach to Freeform Fabrication, *Int. J. Mach. Tools Manuf.*, 2007, **47**(3-4), p 627-634.
15. R.A. Seraj, A. Abdollah-zadeh, S. Dosta, H. Canales, H. Assadi and I.G. Cano, The Effect of Traverse Speed on Deposition Efficiency of Cold Sprayed Stellite 21, *Surf. Coat. Technol.*, 2019, **366**, p 24-34.
16. Z. Arabgol, M. Villa Vidaller, H. Assadi, F. Gärtner and T. Klassen, Influence of Thermal Properties and Temperature of Substrate on the Quality of Cold-Sprayed Deposits, *Acta Mater.*, 2017, **127**, p 287-301.
17. A.W.-Y. Tan, W. Sun, Y.P. Phang, M. Dai, I. Marinescu, Z. Dong and E. Liu, Effects of Traverse Scanning Speed of Spray Nozzle on the Microstructure and Mechanical Properties of Cold-Sprayed Ti6Al4V Coatings, *J. Therm. Spray Tech.*, 2017, **26**(7), p 1484-1497.
18. K. Taylor, B. Jodoin and J. Karov, Particle Loading Effect in Cold Spray, *J. Therm. Spray Tech.*, 2006, **15**(2), p 273-279.
19. O.C. Ozdemir, C.A. Widener, M.J. Carter and K.W. Johnson, Predicting the Effects of Powder Feeding Rates on Particle Impact Conditions and Cold Spray Deposited Coatings, *J. Therm. Spray Tech.*, 2017, **26**(7), p 1598-1615.
20. C. Chen, S. Gojon, Y. Xie, S. Yin, C. Verdy, Z. Ren, H. Liao and S. Deng, A Novel Spiral Trajectory for Damage Component Recovery with Cold Spray, *Surf. Coat. Technol.*, 2017, **309**, p 719-728.
21. The FreeCAD Team, Freecad (Version 0.20). <https://www.freecadweb.org/>. Accessed November 03, 2022.
22. RoboDK Inc., Robodk (Version 5.5.0). <https://robodk.com/>. Accessed November 03, 2022.
23. H. Wu, S. Liu, W. Li, M. Lewke, R.-N. Raoelison, A. List, F. Gärtner, H. Liao, T. Klassen and S. Deng, Generic Implementation of Path Design for Spray Deposition: Programming Schemes, Processing and Characterization for Cold Spraying, *Surf. Coat. Technol.*, 2023, **458**, 129368.
24. A. Nardi, D. Helfritsch, O.C. Ozdemir, and V.K. Champagne, Process Control, *Practical Cold Spray*, V.K. Champagne Jr., O.C. Ozdemir, and A. Nardi, Eds., Springer International Publishing, 2021, p 265-284.
25. K.J. Waldron and J. Schmiedeler, Kinematics, *Springer Handbook of Robotics*. B. Siciliano, O. Khatib Ed., Springer International Publishing, Heidelberg, New York, 2016, p 11-36

**Publisher’s Note** Springer Nature remains neutral with regard to jurisdictional claims in published maps and institutional affiliations.